High-fidelity photon-subtraction operation for large-photon-number Fock states

Shengli Zhang [*]
Beijing Key Laboratory of Nanophotonics & Ultrafine Optoelectronic Systems, School of Physics, Beijing Institute of Technology, 100081 Beijing, China

(Received 10 November 2019; accepted 3 February 2020; published 24 February 2020)

The statistics of photon-subtracted and photon-added states has several important applications in quantum optics and quantum information science. In this study, we propose a scheme for a photon-subtraction operation with SU(1,1) beam splitters. We demonstrate that our scheme overcomes the exponential decaying trend of fidelity and works exceptionally well for quantum states with a large number of photons. Moreover, our scheme is effective even with realistic on-off photon detectors and the heralded single-photon source. Thus, our scheme can serve as a useful tool for manipulating the number of photons in bright coherent states and strongly squeezed states in the future.

DOI: 10.1103/PhysRevA.101.023835

I. INTRODUCTION

Photon annihilation $\hat{a}$ and photon creation $\hat{a}^{\dagger}$ are two widely used noncommutative operations in quantum optics [1], with several applications in continuous-variable quantum information processing [2]. For example, these operators have been applied in fundamental tests for noncommutation [3], quantum illumination with low error probability [4,5], continuous-variable entanglement distillation [6,7], high-fidelity noiseless amplifier [8], coherence-preserving non-Gaussian quantum channel [9], Bell-inequality violation with non-Gaussian entanglement [10,11], and continuous-variable Bose sampling [12].

The ideal photon-annihilation and -creation operations are nonphysical operations, and realistic schemes for these operations have been implemented with conventional beam splitters (BSs) and photon detectors [13–15]. Nevertheless, all of these schemes are restricted to weak input states within few-photon subspace ($|\psi\rangle = \sum_{i=0}^{D-1} c_i|i\rangle$, $D \ll 10$). Consequently, the realization of photon-annihilation and -creation operations for large-photon-number subspace is missing. However, the recent breakthrough in the preparation of a single-mode squeezed vacuum state has entered a regime of 15 dB [16]. Here, the average number of photons was $\bar{n} = 7.41$ and a 70-dimensional subspace of $|0\rangle, |1\rangle, \ldots, |69\rangle$ was required to simulate the non-negligible population. The photon-annihilation and -creation operations, originally designed for a small photon population, are not adequate for Fock states with a large number of photons. In this study, we propose a scheme using a SU(1,1) beam splitter (SBS) to realize single-photon subtraction for large Fock states.

Recently, SBS has garnered considerable attention in quantum metrology for enhancing the robustness [17,18] and precision [19–22]. Actually, the study of SBS dates back to the 1980s. Yurke *et al.* [23] introduced a new class of interferometer in 1986, which could be characterized by the SU(1,1) group. This interferometer can be implemented with active lossless devices such as four-wave mixers. Subsequently, Brief and Mann showed that a SU(1,1) interferometer could be used to enhance the phase sensitivity [24]. Moreover, it has been shown that the phase measurement with SBS can even achieve a precision that scales as the Heisenberg limit [25]. Incidentally, in a separate line of research, the SU(1,1) group has also triggered a number of studies for the so-called intelligent state, which minimizes the uncertainly relations for the Hermitian generators of the related Lie group [26–32].

Here, we show that the proposed SBS-based scheme can surmount the exponential decaying trend of fidelity in the photon-subtraction operation, which is often observed with conventional BS. Thus, our scheme provides a powerful tool for realizing the photon subtraction of large Fock states ($N \sim 100$).

The rest of this paper is organized as follows. Section II shows the basic schemes of photon subtraction based on conventional BS and SBS. In Sec. III, we use the superposition state, bright coherent state, and strongly squeezed vacuum state as three examples to analyze the performance of the proposed SBS-based photon-subtraction scheme. Section IV is devoted to the performance analysis when the ideal single-photon detectors are replaced with on-off photon detectors. The robustness of the proposed scheme with a realistic single-photon source is validated in Sec. V. Section VI is devoted to a detailed analysis of the SBS-based scheme in the presence of detector inefficiency and dark-count rate. Finally, the study is concluded in Sec. VII.

II. PHOTON-SUBTRACTION OPERATION FOR FOCK STATES WITH SMALL AND LARGE NUMBER OF PHOTONS

Figure 1(a) shows the existing scheme of photon subtraction for a Fock state with a small number of photons, which is implemented using a conventional BS with transmittance T. Here, photon subtraction is a probabilistic operation. The operation is successful if the detector registers a single-photon count.

*zhangshengli@bit.edu.cn

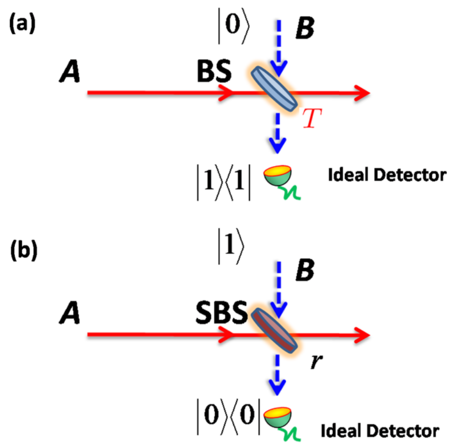

FIG. 1. (a) Schematic of photon-subtraction operation with a conventional BS and single-photon detector. (b) Schematic of photon-subtraction operation for a large-photon-number Fock state with SBS and single-photon ancilla. BS denotes the conventional beam splitter with transmittance T and SBS denotes the SU(1,1) beam splitter with parameter r.

For convenience, we start with the Fock state $|\psi\rangle = |n\rangle$. The coupling between $|n\rangle$ and vacuum state $|0\rangle$ can be expressed as

$$|\psi^{(a)}\rangle_{\rm AB} = U_{\rm BS}(T)|n\rangle|0\rangle = e^{\theta_0(\hat{a}\hat{b}^\dagger - \hat{a}^\dagger\hat{b})}|n\rangle|0\rangle, \tag{1}$$

where $\theta_0 = \arctan[\sqrt{(1-T)/T}]$, $\hat{a}$ and $\hat{b}$ are photon-annihilation operators for the two interacting optical modes. After direct calculation, we obtain [33]

$$|\psi^{(a)}\rangle_{\rm AB} = \sum_{k=0}^{n}\sqrt{\binom{n}{k}}(T)^{\frac{n-k}{2}}(1-T)^{\frac{k}{2}}|n-k\rangle_A|k\rangle_B. \tag{2}$$

The state $|\psi^{(a)}\rangle_{\rm AB}$ is a superposition of $|n-k,k\rangle$. If $k=1$, then one sees that the corresponding optical mode A is now left to the $|n-1\rangle$ state. Actually, this is the working principle of the conventional scheme for photon subtraction. Mathematically, this can be expressed as a nonunitary transformation,

$$|n\rangle \to_B \langle 1|\psi^{(a)}\rangle_{\rm AB} = g_1(n)|n-1\rangle, \tag{3}$$

where

$$g_1(n) = \sqrt{\frac{n(1-T)}{T}}T^{\frac{n}{2}}. \tag{4}$$

Thus, a single photon is subtracted from the input Fock state $|n\rangle$. For a pure Fock state $|n\rangle$, the coefficient $g_1(n)$ can be canceled by normalization. However, for a superposition state $|\psi\rangle = \sum_n c_n|n\rangle$, the output state (before normalization) follows $|\psi'\rangle = \sum_n c_n g_1(n)|n-1\rangle$. For $0<T<1$, an exponentially decaying term $T^{n/2}$ rapidly decreases the fidelity of the actual photon-subtraction operation.

We now focus on the SBS-based scheme shown in Fig. 1(b). Here, an ancillary single-photon state is required. In contrast to the earlier scheme, the zero-photon count in the detector is enough to herald a successful photon-subtraction operation. Here also, we assume that the input Fock state is $|\psi\rangle = |n\rangle$ for simplicity. Now, the coupling can be given by

$$|\psi^{(b)}\rangle_{\rm AB} = U_S(r)|n\rangle_A|1\rangle_B, \tag{5}$$

where $U_S(r) = e^{r(\hat{a}^\dagger\hat{b}^\dagger - \hat{a}\hat{b})}$. Using straightforward algebra, we obtain

$$U_S(r)\hat{a}^\dagger U_S(r)^\dagger = \hat{a}^\dagger\cosh(r) - b\sinh(r), \tag{6}$$

$$U_S(r)\hat{b}^\dagger U_S(r)^\dagger = \hat{b}^\dagger\cosh(r) - \hat{a}\sinh(r), \tag{7}$$

and

$$|\psi^{(b)}\rangle_{\rm AB} = \frac{1}{\sqrt{n!}}[U_S(r)\hat{a}^\dagger U_S(r)^\dagger]^n U_S(r)\hat{b}^\dagger U_S(r)^\dagger|\psi_{00}\rangle, \tag{8}$$

where $|\psi_{00}\rangle = U_S(r)|00\rangle = \sum_{p=0}^{\infty}\sqrt{1-\lambda^2}\lambda^p|p\rangle|p\rangle$ is the two-mode squeezed vacuum state and $\lambda = \tanh(r)$ is the squeezing parameter. Using Eqs. (6)–(8), we get

$$\begin{aligned}|\psi^{(b)}\rangle_{\rm AB} &= \sum_{p=0}^{\infty}\frac{\sqrt{1-\lambda^2}}{\sqrt{n!}}\sum_{k=0}^{n}h_1(n,k,p)|p+k,p+1-(n-k)\rangle\rangle \\ &\quad + \sum_{p'=0}^{\infty}\frac{\sqrt{1-\lambda^2}}{\sqrt{n!}}\sum_{k=0}^{n}h_2(n,k,p')|p'+k-1,p'-(n-k)\rangle,\end{aligned} \tag{9}$$

where

$$h_1(n,k,p) = \lambda^p\binom{n}{k}\cosh(r)^{k+1}[-\sinh(r)]^{n-k}(p+1) \times\sqrt{\frac{(p+k)!}{[p+1-(n-k)]!}}, \tag{10}$$

$$h_2(n,k,p') = \lambda^{p'}\binom{n}{k}\cosh(r)^{k}[-\sinh(r)]^{n-k+1}p' \times\sqrt{\frac{(p'+k-1)!}{[p'-(n-k)]!}}. \tag{11}$$

From Eq. (9), it follows that $|\psi^{(b)}\rangle_{\rm AB}$ is a superposition,

$$c_0|n-1\rangle_A|0\rangle_B + c_1|n\rangle_A|1\rangle_B + c_2|n+1\rangle_A|2\rangle_B + |n+2\rangle_A|3\rangle_B\cdots \tag{12}$$

Thus, if we project the optical mode B to $|0\rangle$, we obtain a state, i.e., $|n-1\rangle_A$ in optical mode A, which is the single-photon-subtracted state if $|n\rangle$ is the input state in optical mode A. Mathematically, by setting $p=n-k-1$ and $p'=n-k$, one obtains

$$\begin{aligned}{}_B\langle 0|\psi^{(b)}\rangle_{\rm AB} &= \frac{\sqrt{1-\lambda^2}}{\sqrt{n!}}[h_1(n,k,n-k-1)+h_2(n,k,n-k)] \\ &= g_2(n)|n-1\rangle,\end{aligned} \tag{13}$$

where

$$g_2(n) = \sum_{k=0}^{n}\binom{n}{k}\frac{n-k}{\sqrt{n}}(-1)^{n-k}\sinh(r)^{2n-1-2k}\cosh(r)^{2k-n-1}. \tag{14}$$

It may be noted that we have only considered the case in which the optical mode B is projected to a vacuum state.

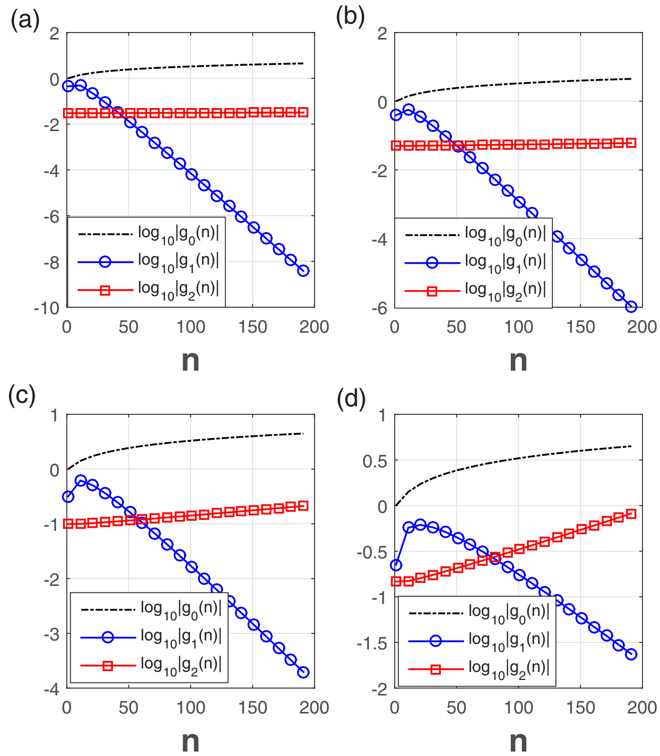

FIG. 2. $g_0(n) = \sqrt{n}$, $g_1(n)$, and $g_2(n)$ (in logarithmic scale) as a function of the number of photons (n). Remaining parameters: (a) $T = 0.80$, $r = 0.03$; (b) $T = 0.85$, $r = 0.05$; (c) $T = 0.90$, $r = 0.10$; (d) $T = 0.95$, $r = 0.15$.

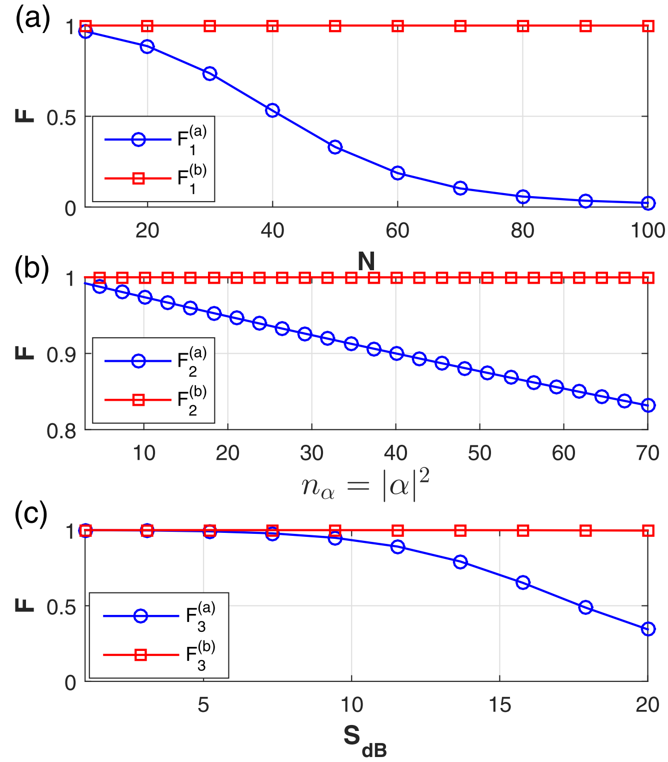

FIG. 3. Fidelity for ideal photon subtraction on a (a) superposition state [Eq. (15)], (b) bright coherent state [Eq. (18)], and (c) strong single-mode squeezed vacuum state [Eq. (19)]. Other parameters: $T = 0.90$ and $r = 0.05$. Photons in each mode are truncated within a 200-dimensional subspace of $\{|0\rangle, |1\rangle, \ldots, |199\rangle\}$ for numerical convergence and computation feasibility.

Actually, there are some other cases as well in which B is projected to a nonvacuum state. Thus, our photon subtraction is a probabilistic postselection process, selecting only the case in which B is projected to the $|0\rangle$ state.

$g_2(n)$ is affected by two interesting trends. First, $\sinh(r)^{2n-1-2k}$ ($r \ll 1$) exponentially decreases for $k \lesssim n$, where n is very large. Second, $\cosh(r)^{2k-n-2}$ and the binomial coefficient $\binom{n}{k}$ exponentially increase for $k \gtrsim n/2$, where n is large. These two contradicting effects finally result in a slowly varying function $g_2(n)$.

Figure 2 compares the values of $g_1(n)$ and $g_2(n)$ (in logarithmic scale) for typical combinations of T and r. The ideal photon subtraction $\hat{a}|n\rangle = \sqrt{n}|n-1\rangle \equiv g_0(n)|n-1\rangle$ is represented with black dotted lines. $g_1(n)$ decays exponentially for all values of T (0.80, 0.85, 0.90, and 0.95). However, for $r \sim 0.03$–0.10, a slowly varying trend of $g_2(n)$ is observed. This proves that the SBS-based scheme is a viable candidate to realize photon subtraction for a large photon population.

III. EXAMPLES OF PHOTON-SUBTRACTION OPERATION

The slowly varying term $g_2(n)$ provides some insights to implement the photon-subtraction operation in the regime of large-photon-number Fock states. We now consider a superposition state, bright coherent state, and strongly squeezed vacuum state as examples for investigating the performance of the proposed scheme in realistic scenarios.

A. Superposition states

Let us start with an equal superposition state,

$$|\psi_1\rangle = \frac{1}{\sqrt{2}}(|1\rangle + |N+1\rangle). \tag{15}$$

After ideal photon subtraction and normalization, we obtain

$$|\psi_1^{\text{out}}\rangle = \frac{\hat{a}|\psi_1\rangle}{\sqrt{\langle\psi_1|\hat{a}^\dagger\hat{a}|\psi_1\rangle}} = \frac{|0\rangle + \sqrt{N+1}|N\rangle}{\sqrt{N+2}}. \tag{16}$$

Here, the schemes shown in Figs. 1(a) and 1(b) are used to perform the photon-subtraction operation on $|\psi_1\rangle$. Let the output states (after normalization) be $|\psi_1^{(a)\text{out}}\rangle$ and $|\psi_1^{(b)\text{out}}\rangle$, respectively. The performance of these two schemes can be evaluated in terms of fidelity, which is defined as follows:

$$F_1^{(a)} = |\langle\psi_1^{\text{out}}|\psi_1^{(a)\text{out}}\rangle|^2, \quad F_1^{(b)} = |\langle\psi_1^{\text{out}}|\psi_1^{(b)\text{out}}\rangle|^2. \tag{17}$$

Figure 3(a) illustrates the variation of $F_1^{(a)}$ and $F_1^{(b)}$ as a function of N. The fidelity for the scheme of Fig. 1(b) outperforms that of Fig. 1(a). Consider the superposition state $|\psi_1\rangle(N = 60)$ as an example. For the scheme in Fig. 1(a) with conventional BS and $T = 0.90$, an ideal single-photon detection in mode B projects the state in mode A to ${}_B\langle 1|U_{\text{BS}}(T)|\psi_1\rangle|0\rangle = \frac{1}{\sqrt{2}}\{[\langle 0|\langle 1|U_{\text{BS}}(T)|1\rangle|0\rangle]|0\rangle + [\langle 60|\langle 1|U_{\text{BS}}(T)|61\rangle|0\rangle]|1\rangle\} = \sqrt{\frac{1-T}{2}}[|0\rangle + \sqrt{61}(T^{30})|60\rangle] \propto (|0\rangle + \sqrt{61} \times 0.0424|60\rangle)$. It is clear that the term $T^{30} = 0.90^{30} =$

0.0424 significantly reduces the coefficient of $|60\rangle$. After normalization, the fidelity $F_1^{(a)} = 0.1847$. However, if a nonlinear BS with $r = 0.05$ is used, the projection of optical mode B to $|0\rangle$ induces a state ${}_B\langle 0|U_S(r)|\psi_1\rangle|1\rangle = \frac{1}{\sqrt{2}}\{[\langle 0|\langle 0|U_S(r)|1\rangle|1\rangle]|0\rangle + [\langle 60|\langle 0|U_S(r)|61\rangle|1\rangle]|1\rangle\} = \frac{1}{\sqrt{2}}(0.0499|0\rangle + 0.3616|60\rangle) \propto (|0\rangle + \sqrt{61} \times 0.9288|60\rangle)$, which gives a fidelity $F_1^{(b)}$ of 0.9998 with respect to $|\psi_1^{\text{out}}\rangle$. Furthermore, even for superposition of the higher Fock state with $N = 100$, a high fidelity, i.e., $F_1^{(b)} > 0.9990$, can be obtained.

B. Bright coherent states

The coherent state, also called the "Glauber coherent state" [34], plays a vital role in quantum optics. It is the eigenstate of the annihilation operation $\hat{a}|\alpha\rangle = \alpha|\alpha\rangle$. In the Fock-state basis, a coherent state can be written as

$$|\alpha\rangle = \sum_{n=0}^{\infty} \frac{e^{-|\alpha|^2/2}\alpha^n}{\sqrt{n!}}|n\rangle. \tag{18}$$

Here, we assume that $|\psi_2\rangle = |\alpha\rangle$ and that the ideal photon-subtraction operation generates $|\psi_2^{\text{out}}\rangle = |\psi_2\rangle = |\alpha\rangle$. The photon-subtraction operation with the schemes of Figs. 1(a) and 1(b) generates $|\psi_2^{(a)\text{out}}\rangle$ and $|\psi_2^{(b)\text{out}}\rangle$, respectively. Figure 3(b) shows the corresponding fidelities $F_2^{(a)}$ and $F_2^{(b)}$ as a function of the average photon number, $n_\alpha = |\alpha|^2$. Numerical calculations show that the proposed scheme for photon subtraction works exceptionally well even for bright coherent states ($F_2^{(b)} = 0.9999$, $n_\alpha = 70$).

C. Strong single-mode squeezed vacuum state

Recently, a strong single-mode squeezed vacuum state at 15 dB classical noise was successfully generated [16]. It is quite interesting to investigate the performance and fidelity of the SBS-based photon-subtraction scheme for a single-mode squeezed vacuum state. We assume that

$$|\psi_3\rangle = \frac{1}{\sqrt{\cosh(r')}} \sum_{k=0}^{\infty} \frac{\sqrt{(2k)!}}{k!}\left[\frac{\tanh(r')}{2}\right]^k |2k\rangle. \tag{19}$$

The squeezing of $|\psi_3\rangle$ (measured in dB) and the average photon number are expressed as

$$S_{\text{dB}} = 20r\log_{10} e, \quad \langle n\rangle = \sinh(r')^2. \tag{20}$$

The corresponding fidelities $F_3^{(a)}$ and $F_3^{(b)}$ are numerically evaluated for varying squeezing levels. As shown in Fig. 3(c), the fidelity of the conventional BS-based scheme decreases rapidly when the squeezing (dB) is linearly increased. However, the SBS-based scheme is efficient even for a strong squeezing regime (e.g., $F_3^{(b)} = 0.9968$ for 20 dB squeezing).

IV. SCHEME WITH ON-OFF PHOTON DETECTORS

The scheme in Fig. 1(a) requires a single-photon detector to identify a single-photon state $|1\rangle$ in the ancillary optical mode. The scheme in Fig. 1(b) requires an additional single-photon source. Here, we compare the performance of these two schemes by replacing the photon detectors in Fig. 1 with more realistic on-off photon detectors. The on-off photon detectors just provide "on" and "off" results, indicating the detection of one or more photons and no photons, respectively [35].

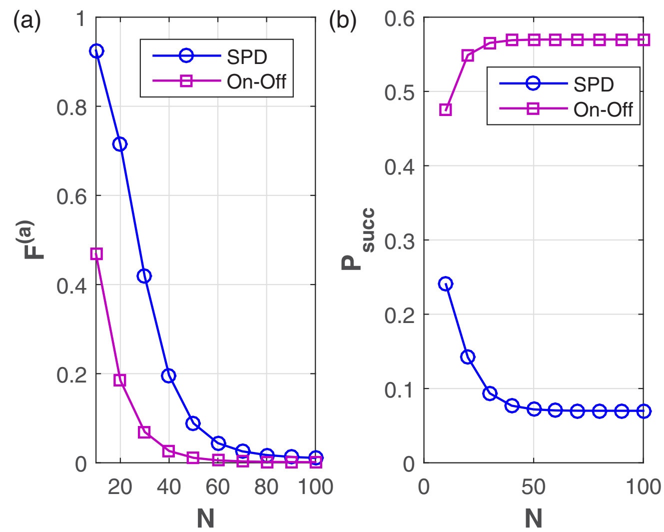

FIG. 4. (a) Fidelity and (b) success probability of the photon-subtraction operation in Fig. 1(a). SPD denotes the ideal single-photon detector and on-off denotes the on-off photon detectors. Photons in each mode are truncated within a 200-dimensional subspace. Here, $T = 0.86$.

The successful photon subtraction for the scheme in Fig. 1(a) is realized if the relevant photon detector registers an "on" result. Physically, the "on" result projects the ancillary optical mode on the nonvacuum subspace, and the output state is a mixed state, which can be expressed as

$$\rho_A^{(a)} = \rho_{A,\text{reduce}}^{(a)}/P_{\text{succ}}, \quad P_{\text{succ}} = \text{Tr}\big[\rho_{A,\text{reduce}}^{(a)}\big], \tag{21a}$$

$$\rho_{A,\text{reduce}}^{(a)} = \text{Tr}_B[|\psi_{\text{AB}}\rangle\langle\psi_{\text{AB}}|(I \otimes \hat{\Pi}_{(\text{on})})], \tag{21b}$$

where $\hat{\Pi}_{(\text{on})} = I - |0\rangle\langle 0| = \sum_{k=1}^{\infty}|k\rangle\langle k|$, and $\text{Tr}_B[\cdot]$ is the partial trace of the optical mode B. $|\psi_{\text{AB}}\rangle = |\psi\rangle \otimes |0\rangle$ is a Kronecker product of the state being photon subtracted and vacuum ancilla. The fidelity of our scheme is defined as $F = \langle\psi^{\text{out}}|\rho_A|\psi^{\text{out}}\rangle$, where $|\psi^{\text{out}}\rangle = \hat{a}|\psi\rangle/\sqrt{\langle\psi|\hat{a}^\dagger\hat{a}|\psi\rangle}$ is the output of the ideal photon subtraction. It should be noted that the performance of the scheme in Fig. 1(a) is strongly affected by the on-off detectors because, for a large number of photons, more photons arrive at the BSs and are directed to these detectors. The contribution of the $|2\rangle\langle 2|, |3\rangle\langle 3|, |4\rangle\langle 4|, \ldots$ states is also registered by the on-off detector. Therefore, the "on" result in such a detector cannot be attributed to a pure $|1\rangle\langle 1|$ projection.

Figure 4 shows the degradation of fidelity in the conventional BS-based scheme [Fig. 1(a)] to realize the subtraction of a single photon from the superposition state in Eq. (15). It is evident that the fidelity degrades significantly when the ideal single-photon detector is replaced with an on-off detector. However, such a loss of fidelity is accompanied by an increase in the success probability.

The successful photon subtraction for the scheme in Fig. 1(b) is realized if the on-off photon detector registers the "off" result. Mathematically, we have

$$\rho_A^{(b)} = \rho_{A,\mathrm{reduce}}^{(b)}/P_{\mathrm{succ}}, \quad P_{\mathrm{succ}} = \mathrm{Tr}\big[\rho_{A,\mathrm{reduce}}^{(b)}\big], \tag{22a}$$

$$\rho_{A,\mathrm{reduce}}^{(b)} = \mathrm{Tr}_B[U_S(r)(|\psi\rangle\langle\psi| \otimes |1\rangle\langle 1|)U_S(r)^\dagger(I \otimes \hat{\Pi}_{(\mathrm{off})})], \tag{22b}$$

where $\hat{\Pi}^{(\mathrm{off})} = |0\rangle\langle 0|$, and $\mathrm{Tr}_B[\cdot]$ denotes taking the partial trace of the optical mode B. $|\psi\rangle$ is again the state being photon subtracted. $\rho_{A,\mathrm{reduce}}^{(b)}$ is the unnormalized state and the normalization factor of $\rho_{A,\mathrm{reduce}}^{(b)}$ is the probability of successful photon subtraction.

It is clear from Eq. (22b) that the projection on $\hat{\Pi}^{(\mathrm{off})}$ in the practical scheme with the on-off detector is exactly the same as that on $|0\rangle\langle 0|$ in the single-photon detector scheme [Fig. 1(b)]. Therefore, the fidelity of the proposed SBS-based scheme is not degraded if the single-photon detector is replaced with the on-off photon detector.

V. SCHEME WITH NONIDEAL SINGLE-PHOTON SOURCE

The SBS-based scheme requires an additional single-photon source. It is quite interesting to investigate the performance of photon subtraction in the presence of a nonideal single-photon source. Equation (22b) is still valid here, except that the ideal single-photon state $|1\rangle\langle 1|$ is replaced by a mixed state ρ_B, which is the density matrix of a realistic single-photon source.

Several single-photon sources using single emitters such as a single atom [36,37], single molecule [38], nitrogen-vacancy center [39,40], and semiconductor quantum dot [41] have been proposed and experimentally verified. Here, we focus on a heralded single-photon source, which is generated by a two-mode squeezed state. Such states have been widely used in quantum cryptography [42–46] and quantum information processing [47,48]. The density matrix for a heralded single-photon source is

$$\rho_B = \sum_{k=1}^{\infty}(1-\lambda'^2)\lambda'^{(2k-2)}|k\rangle\langle k|, \tag{23}$$

where $0 < \lambda' < 1$ is a parameter related to the squeezing in the photon-number correlated state. For $\lambda' \to 0$, $\rho_B \to |1\rangle\langle 1|$ is the true single-photon state. For $\lambda' > 0$, a multiphoton state contributes to ρ_B, which degrades the fidelity of the SBS-based photon-subtraction scheme. This is because a multiphoton state in ρ_B, say $|2\rangle\langle 2|$, definitely generates two-photon subtraction, which is clear from

$$\begin{aligned}&\mathrm{Tr}_B[U_S(r)(|n\rangle\langle n| \otimes |2\rangle\langle 2|)U_S(r)^\dagger(I \otimes \hat{\Pi}_{(\mathrm{off})})]\\ &\quad = \widetilde{g}^{(2)}(n)|n-2\rangle\langle n-2|.\end{aligned} \tag{24}$$

Thus, two-photon subtraction can also occur along with single-photon subtraction in the final output. Figure 5 shows the evaluated fidelity of photon subtraction for different values of λ'. As expected, the fidelity degrades slightly as λ' increases. However, the fidelity of the SBS-based scheme is still high ($F_2^{(b)} = \langle\psi_1^{\mathrm{out}}|\rho_{A,\mathrm{reduce}}^{(b)}|\psi_1^{\mathrm{out}}\rangle = 0.9888$ for $N = 100$ and $\lambda' = 0.3$). Moreover, the success probability is negligibly affected due to the heralded single-photon state.

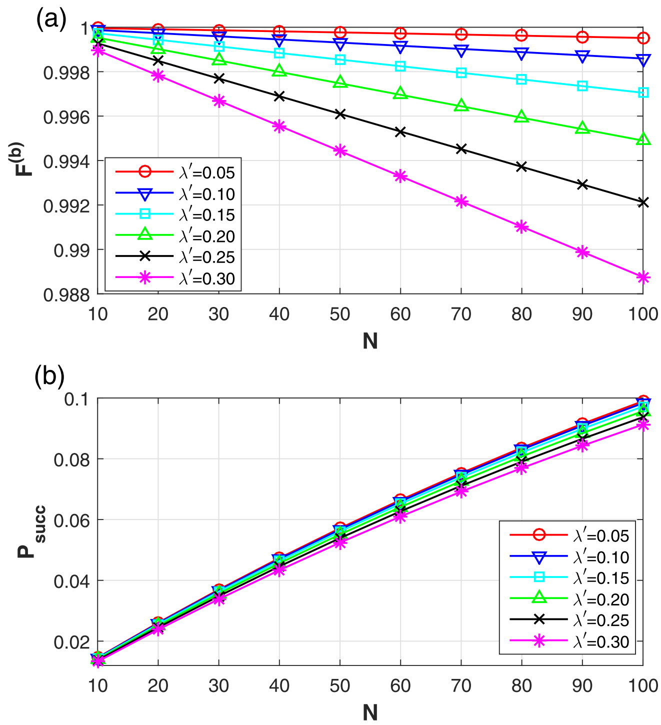

FIG. 5. (a) Fidelity and (b) success probability of the photon-subtraction operation with more realistic dichotic on-off photon detectors and heralded single-photon source for varying λ'. The input state to be photon subtracted is the superposition state given by Eq. (15). From top to bottom: $\lambda' = 0.05, 0.10, 0.15, 0.20, 0.25, 0.30$. Photons in each mode are truncated within a 200-dimensional subspace. Here, $r = 0.05$.

VI. PRACTICALITY OF THE SCHEME: SBS WITH WEAK COUPLING AND PHOTON DETECTOR WITH DARK-COUNT RATE

For a detailed analysis of the practical applications of our scheme, we consider a scenario where SBS with weak coupling and photon detector with dark-count rate are used. Experimentally, a SBS can be implemented with optical parametric amplification (OPA) [18,22,49–51]. A recent experimental study using a Mach-Zehnder (MZ) interferometer with SBS has demonstrated an improvement of 4.1 dB in the signal-to-noise ratio compared with that in a conventional interferometer under the same operating conditions [51].

Hudelist *et al.* [51] realized an OPA experiment with a gain of $G = \cosh(r) = 1.6583$ using a Rb-85 vapor cell. This corresponds to $r = 1.0923$. However, in our scheme, we do not need such a high gain. A small gain, i.e., $G = \cosh(0.05) = 1.0013$, is sufficient. Thus, in principle, our scheme can be implemented with weak processes such as parametric down conversion [52].

Detection efficiency and dark counts are other factors that should be considered for a realistic photon-subtraction scheme. The proposed scheme is more efficient if the detector

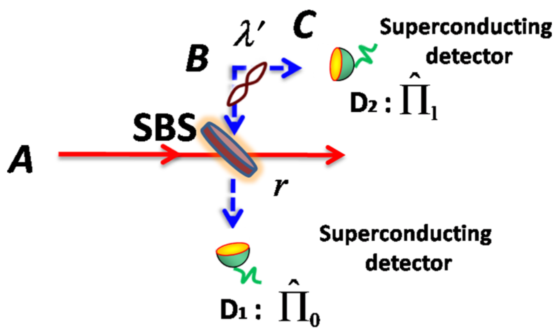

FIG. 6. Realistic scheme of photon subtraction with a conventional superconducting detector. λ' represents the parameter for a heralded single-photon state in optical mode B. $\hat{\Pi}_0$ and $\hat{\Pi}_1$ are the elements of the POVM for the superconducting detector.

that is employed has a high quantum efficiency. We now focus our attention on the superconducting detector.

Superconducting nanowire single-photon detectors (SNSPDs) exhibit several advantages, including high detection efficiency, low dark-count rate, and low time jitter. This provides us with a chance to evaluate the practical performance of our scheme with state-of-the-art commercial equipment. A schematic of our photon-subtraction scheme is shown in Fig. 6, where we assume that the heralded single photon and the projection to vacuum state $|0\rangle\langle 0|$ are implemented by two independent SNSPDs.

According to quantum measurement theory [53,54], a SNSPD with nonunity detection efficiency η and dark count ν can be expressed by positive operator-valued measure (POVM) [55],

$$\hat{\Pi}_n = \sum_{m=n}^{\infty} \Pi_{nm}|m\rangle\langle m|, \tag{25}$$

$$\Pi_{nm} = e^{-\nu}\sum_{j}\frac{\nu^j}{j!}B_{(n-j)m}, \tag{26}$$

$$B_{nm} = \binom{m}{n}\eta^n(1-\eta)^{m-n}, \tag{27}$$

$$n = 0, 1, 2, \ldots. \tag{28}$$

Here, dark counts indicate the registered counts without any incident photon. In this paper, we have assumed that dark counts follow Poissonian statistics with mean number ν. For example, if we consider a SNSPD, the typical parameters for detecting a single photon at 800 nm are $\eta \geqslant 0.95$ and $\nu \leqslant 1 \times 10^{-7}$ [56].

In this case, the heralded single photon is generated when D_2 registers "1" as the result. This is mathematically equivalent to projecting the relevant optical mode C to $\hat{\Pi}_1$. Similar to Fig. 1(b), successful photon subtraction happens when D_1 registers a "0" result.

The output state after photon subtraction with a superconducting detector is given by

$$\rho_A^{(\mathrm{SBS})} = \frac{1}{P_{01}}\mathrm{Tr}_{BC}\big[U_S|\psi_{\mathrm{tot}}\rangle\langle\psi_{\mathrm{tot}}|U_S^{\dagger}\big(\hat{\Pi}_0^{(B)} \otimes \hat{\Pi}_1^{(C)}\big)\big], \tag{29}$$

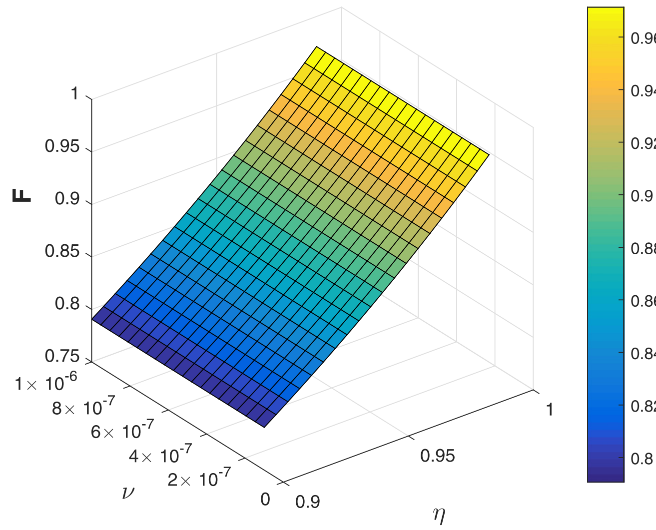

FIG. 7. Fidelity of SBS-based photon subtraction on $|\psi_1\rangle$ ($N = 100$) as a function of detection efficiency η and dark count ν. Other parameters: $\lambda' = 0.05$ and $r = 0.10$. All photons are truncated within 200-dimensional subspace spanned by $\{|0\rangle, |1\rangle, |2\rangle, \ldots, |199\rangle\}$.

where

$$P_{01} = \mathrm{Tr}\big[U_S|\psi_{\mathrm{tot}}\rangle\langle\psi_{\mathrm{tot}}|U_S^{\dagger}\big(\hat{\Pi}_0^{(B)} \otimes \hat{\Pi}_1^{(C)}\big)\big], \tag{30}$$

and $|\psi_{\mathrm{tot}}\rangle$ is the initial state of optical modes A and $B-C$, which is expressed as

$$|\psi_{\mathrm{tot}}\rangle = |\psi\rangle \otimes \sum_{k=0}^{\infty}\sqrt{1-\lambda'^2}\lambda'^k|k\rangle|k\rangle. \tag{31}$$

Here, we consider the superposition state $|\psi_1\rangle$ [Eq. (15), $N = 100$] as the input state. The output state for ideal photon subtraction is $|\psi_1^{\mathrm{out}}\rangle = 0.0990|0\rangle + 0.9950|100\rangle$. As an example, we use the scheme in Fig. 6 with SBS implemented by OPA where gain $G = \cosh(0.05) = 1.0013$ and the single photon is heralded with parameter $\lambda' = 0.05$. Parametric down conversion with $\lambda' = 0.05$ can be implemented according to the recent advancement in experimental techniques [57]. The fidelity of the heralded single photon in the outgoing mode B is $1-\lambda'^2$. Thus, a weaker parametric down conversion can induce a higher fidelity for an ideal single-photon state.

The performance of our photon-subtraction scheme as a function of detection efficiency η and dark count ν is shown in Fig. 7. It is evident that the fidelity of our scheme is severely affected by the detector inefficiency. This is because the success of our photon-subtraction scheme relies on the projection of the ancillary outgoing mode B to vacuum mode $|0\rangle\langle 0|$. However, $|1\rangle\langle 1|$ and $|2\rangle\langle 2|$ are still present in $\hat{\Pi}_0$ [Eq. (25)] because the efficiency $\eta < 1$. This erroneously generates undesired population of the output state in $|1\rangle, |2\rangle, |101\rangle, |102\rangle$ if the initial state is $(|1\rangle + |100\rangle)/\sqrt{2}$. When $\eta = 0.95$ and $\nu = 1.25 \times 10^{-7}$, the output state is $\rho_A^{(\mathrm{SBS})} = 0.0232|0\rangle\langle 0| + 0.1415|0\rangle\langle 100| + 0.1415|100\rangle\langle 0| + 0.8632|100\rangle\langle 100| + 0.1121|1\rangle\langle 1| + 0.0010|102\rangle\langle 102| \cdots$. Here, the populations $|1\rangle\langle 1|$ and $|102\rangle\langle 102|$ are evident, which cause a degradation of fidelity to $F = 0.8828$.

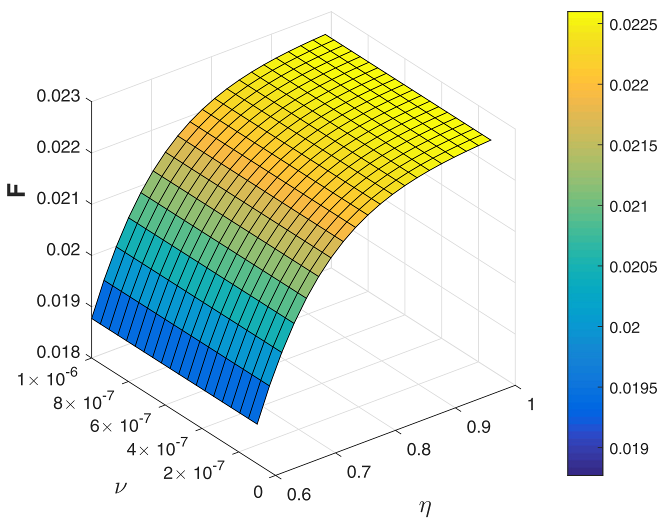

FIG. 8. Fidelity of BS-based photon subtraction on $|\psi_1\rangle$ ($N = 100$) as a function of detection efficiency η and dark count ν. Here, $T = 0.90$. All photons are truncated within 200-dimensional subspace spanned by $\{|0\rangle, |1\rangle, |2\rangle, \ldots, |199\rangle\}$.

Fortunately, our scheme still shows a sharp contrast with the conventional PS scheme. Specifically, if the same SNSPD is used to replace the detector in Fig. 1(a) and to distill the state $|\psi_1\rangle$ with $N = 100$, the output state is given by

$$\rho_A^{(\mathrm{BS})} = \frac{1}{p_{\mathrm{succ}}}\mathrm{Tr}_B[U_{\mathrm{BS}}(|\psi_1\rangle\langle\psi_1| \otimes |0\rangle\langle 0|)U_{\mathrm{BS}}^{\dagger}\hat{\Pi}_1], \quad (32)$$

where $p_{\mathrm{succ}} = \mathrm{Tr}[U_{\mathrm{BS}}(|\psi_1\rangle\langle\psi_1| \otimes |0\rangle\langle 0|)U_{\mathrm{BS}}^{\dagger}\hat{\Pi}_1]$. For $\eta = 0.95$, $\nu = 1.25 \times 10^{-7}$, and $T = 0.90$, we obtain $\rho_A^{(\mathrm{BS})} = 0.9954|0\rangle\langle 0| + 0.0027|100\rangle\langle 100| + 0.0015|99\rangle\langle 99| + 0.0516(|0\rangle\langle 100| + |100\rangle\langle 0|) + \cdots$ and the fidelity is $F = \langle\psi_1^{\mathrm{out}}|\rho_A^{(\mathrm{BS})}|\psi_1^{\mathrm{out}}\rangle = 0.0226$, which is much smaller than that of the SBS-based scheme in Fig. 6. The fidelity of photon subtraction with the scheme in Fig. 1(a) along with SNSPD for different parameters (η, ν) is shown in Fig. 8. Again, the fidelity is almost immune to variation of $\nu : 1 \times 10^{-7}$–1×10^{-6}. It is more sensitive to the detection inefficiency. For $\nu = 1 \times 10^{-6}$, the fidelity decreases from 0.0226 to 0.0188 as η decreases from 0.99 to 0.60. However, the overall fidelity is extremely low compared to that of the SBS-based scheme. This suggests that SBS-based photon subtraction is more efficient for photon subtraction on large Fock states.

VII. CONCLUSIONS

We proposed a SBS-based scheme to implement the photon-subtraction operation for Fock states with a large number of photons. This scheme uses a single-photon ancilla, and its fidelity with the ideal single-photon state is $F \sim 0.99$, even for $N \sim 100$. We also used a bright coherent state and strong single-mode squeezed state as examples to assess the performance of this scheme. Our numerical results confirmed the high fidelity of the SBS-based photon-subtraction operation. Finally, we analyzed the performance of the proposed scheme with more realistic on-off photon detectors, heralded single-photon source, detector inefficiency, and dark-count rate. Our work provides an interesting application of SBS, and we believe that our investigation of the photon-subtraction operation can be further extended to other non-Gaussian operations such as photon creation and photon catalysis [58–60].

ACKNOWLEDGMENTS

This study was funded by the National Natural Science Foundation of China (NSFC Grants No. 11574400 and No. 11204379), Beijing Institute of Technology Research Fund Program for Young Scholars, and the joint program of ICTP (Trieste, Italy) - NSFC (Grant No. 11981240356).

[1] D. F. Walls and G. J. Milburn, *Quantum Optics* (Springer-Verlag, Berlin, 1994).
[2] S. L. Braunstein and P. van Loock, Rev. Mod. Phys. **77**, 513 (2005).
[3] V. Parigi, A. Zavatta, M. Kim, and M. Bellini, Science **317**, 1890 (2007).
[4] S. L. Zhang, J. S. Guo, W. S. Bao, J. H. Shi, C. H. Jin, X. B. Zou, and G. C. Guo, Phys. Rev. A **89**, 062309 (2014).
[5] L. Fan and M. S. Zubairy, Phys. Rev. A **98**, 012319 (2018).
[6] T. Opatrný, G. Kurizki, and D. G. Welsch, Phys. Rev. A **61**, 032302 (2000).
[7] H. Takahashi, J. S. Neergaard-Nielsen, M. Takeuchi, M. Takeoka, K. Hayasaka, A. Furusawa, and M. Sasaki, Nat. Photon. **4**, 178 (2010).
[8] A. Zavatta, Fiurášek, and M. Bellini, Nat. Photon. **5**, 52 (2011).
[9] K. K. Sabapathy and A. Winter, Phys. Rev. A **95**, 062309 (2017).
[10] R. Garcia-Patron, J. Fiurasek, N. J. Cerf, J. Wenger, R. Tualle-Brouri, and P. Grangier, Phys. Rev. Lett. **93**, 130409 (2004).
[11] H. Nha and H. J. Carmichael, Phys. Rev. Lett. **93**, 020401 (2004).
[12] U. Chabaud, T. Douce, D. Markham, P. van Loock, E. Kashefi, and G. Ferrini, Phys. Rev. A **96**, 062307 (2017).
[13] S. Olivares, M. G. A. Paris, and R. Bonifacio, Phys. Rev. A **67**, 032314 (2003).
[14] A. Ourjoumtsev, A. Dantan, R. Tualle-Brouri, and P. Grangier, Phys. Rev. Lett. **98**, 030502 (2007).
[15] N. Namekata, Y. Takahashi, G. Fujii, D. Fukuda, S. Kurimura, and S. Inoue, Nat. Photon. **4**, 655 (2010).
[16] H. Vahlbruch, M. Mehmet, K. Danzmann, and R. Schnabel, Phys. Rev. Lett. **117**, 110801 (2016).
[17] A. M. Marino, N. V. CorzoTrejo, and P. D. Lett, Phys. Rev. A **86**, 023844 (2012).
[18] Y. Liu, J. Li, L. Cui, N. Huo, S. M. Assad, X. Li, and Z. Y. Ou, Opt. Express **26**, 27705 (2018).
[19] L.-L. Guo, Y.-F. Yu, and Z.-M. Zhang, Opt. Express **26**, 29099 (2018).
[20] C. You, S. Adhikari, X. Ma, M. Sasaki, M. Takeoka, and J. P. Dowling, Phys. Rev. A **99**, 042122 (2019).

[21] D. Li, C.-H. Yuan, Z. Y. Ou, and W. Zhang, New J. Phys. **16**, 073020 (2014).
[22] B. E. Anderson, P. Gupta, B. L. Schmittberger, T. Horrom, C. Hermann-Avigliano, K. M. Jones, and P. D. Lett, Optica **4**, 752 (2017).
[23] B. Yurke, S. L. McCall, and J. R. Klauder, Phys. Rev. A **33**, 4033 (1986).
[24] C. Brif and A. Mann, Phys. Rev. A **54**, 4505 (1996)
[25] O. Steuernagel and S. Scheel, J. Opt. B **6**, S66 (2004).
[26] K. Wodkiewicz and J. H. Eberly, J. Opt. Soc. Am. B **2**, 458 (1985).
[27] C. C. Gerry, Phys. Rev. A **31**, 2721 (1985).
[28] G. S. Agarwal and R. R. Puri, Phys. Rev. A **41**, 3782 (1990).
[29] C. Brif and Y. Ben-Aryeh, J. Phys. A **27**, 8185 (1994).
[30] C. Brif and A. Mann, Phys. Lett. A **219**, 257 (1996)
[31] M. M. Nieto and D. R. Truax, Phys. Rev. Lett. **71**, 2843 (1993).
[32] D. A. Trifonov, J. Math. Phys. **35**, 2297 (1994).
[33] S. Zhang and X. Zhang, Phys. Rev. A **97**, 043830 (2018).
[34] R. J. Glauber, Phys. Rev. **131**, 2766 (1963).
[35] A. Kitagawa, M. Takeoka, M. Sasaki, and A. Chefles, Phys. Rev. A **73**, 042310 (2006).
[36] J. McKeever, A. Boca, A. D. Boozer, R. Miller, J. R. Buck, A. Kuzmich, and H. J. Kimble, Science **303**, 1992 (2004).
[37] M. Hijlkema, B. Weber, H. P. Specht, S. C. Webster, A. Kuhn, and G. Rempe, Nat. Phys. **3**, 253 (2007).
[38] F. De Martini, G. Di Giuseppe, and M. Marrocco, Phys. Rev. Lett. **76**, 900 (1996).
[39] C. Kurtsiefer, S. Mayer, P. Zarda, and H. Weinfurter, Phys. Rev. Lett. **85**, 290 (2000).
[40] R. Brouri, A. Beveratos, J.-P. Poizat, and P. Grangier, Opt. Lett. **25**, 1294 (2000).
[41] Z. Yuan, B. E. Kardynal, R. M. Stevenson, A. J. Shields, C. J. Lobo, K. Cooper, N. S. Beattie, D. A. Ritchie, and M. Pepper, Science **295**, 102 (2002).
[42] N. Lütkenhaus, Phys. Rev. A **61**, 052304 (2000).
[43] T. Horikiri and T. Kobayashi, Phys. Rev. A **73**, 032331 (2006).
[44] Y. Adachi, T. Yamamoto, M. Koashi, and N. Imoto, Phys. Rev. Lett. **99**, 180503 (2007).
[45] Q. Wang, W. Chen, G. Xavier, M. Swillo, T. Zhang, S. Sauge, M. Tengner, Z.-F. Han, G.-C. Guo, and A. Karlsson, Phys. Rev. Lett. **100**, 090501 (2008).
[46] N. Montaut, L. Sansoni, E. Meyer-Scott, R. Ricken, V. Quiring, H. Herrmann, and C. Silberhorn, Phys. Rev. Appl. **8**, 024021 (2017).
[47] M. Bellini and A. Zavatta, Prog. Opt. **55**, 41 (2010).
[48] S. L. Zhang, Y. L. Dong, X. B. Zou, B. S. Shi, and G. C. Guo, Phys. Rev. A **88**, 032324 (2013).
[49] J. Jing, C. Liu, Z. Zhou, Z. Y. Ou, and W. Zhang, Appl. Phys. Lett. **99**, 011110 (2011).
[50] M. Manceau, G. Leuchs, F. Khalili, and M. Chekhova, Phys. Rev. Lett. **119**, 223604 (2017).
[51] F. Hudelist, J. Kong, C. Liu, J. Jing, Z. Y. Ou, and W. Zhang, Nat. Commun. **5**, 3049 (2014).
[52] G. Frascella, E. E. Mikhailov, N. Takanashi, R. V. Zakharov, O. V. Tikhonova, and M. V. Chekhova, Optica **6**, 1233 (2019).
[53] E. B. Davies, IEEE Trans. Inf. Theory **24**, 596 (1978).
[54] C. W. Helstrom, *Quantum Detection and Estimation Theory* (Academic, New York, 1976).
[55] G. Brida, L. Ciavarella, I. P. Degiovanni, M. Genovese, L. Lolli, M. G. Mingolla, F. Piacentini, M. Rajteri, E. Taralli, and M. G. A. Paris, New J. Phys. **14**, 085001 (2012).
[56] I. Holzman and Y. Ivry, Adv. Quantum Technol. **2**, 1800058 (2019).
[57] F. Kaneda and P. G. Kwiat, Sci. Adv. **5**, eaaw8586 (2019).
[58] A. I. Lvovsky and J. Mlynek, Phys. Rev. Lett. **88**, 250401 (2002).
[59] K. Sanaka, K. J. Resch, and A. Zeilinger, Phys. Rev. Lett. **96**, 083601 (2006).
[60] L. Hu, Z. Liao, and M. S. Zubairy, Phys. Rev. A **95**, 012310 (2017).